

## Zinc-doped borate bioactive glasses: antibacterial efficacy and environmental application

**Bassant I. Elsaba<sup>1</sup>, Hosam Salaheldin<sup>2</sup>, Yasser S. Rammah<sup>3</sup>, Ashraf Elsayad<sup>1</sup>**

<sup>1</sup> Botany Department, Faculty of Science, Mansoura University, Mansoura 35516, Egypt

(BE [bassantebrahem090@gmail.com](mailto:bassantebrahem090@gmail.com), AE [ashraf-badawy@mans.edu.eg](mailto:ashraf-badawy@mans.edu.eg))

<sup>2</sup> Biophysics Research Group, Physics Department, Faculty of Science, Mansoura University, Mansoura 35516, Egypt (HE [hsmohamed@mans.edu.eg](mailto:hsmohamed@mans.edu.eg))

<sup>3</sup> Department of physics, Faculty of Science, Menoufia University, Shebin El-Koom 32511, Menoufia, Egypt  
(YR [dr\\_yasser1974@yahoo.com](mailto:dr_yasser1974@yahoo.com))

\* **Correspondence to:** Email: [bassantebrahem090@gmail.com](mailto:bassantebrahem090@gmail.com), Tel: 01007127812

Received: 17/7/2024  
Accepted: 29/7/2024

**Abstract:** Reusing of the treated sewage wastewater is addressed as a significant alternative water source in the new water management strategies of Middle Eastern countries and other countries facing water resource shortages. By using the traditional melt-quenching procedure, borate bioactive glasses (BBAGs) doped with varying amounts of zinc oxide (ZnO) (ZnXs) were created. The used composition was (75-X) B<sub>2</sub>O<sub>3</sub>, 10 Na<sub>2</sub>O, 5 P<sub>2</sub>O<sub>5</sub>, 10 Li<sub>2</sub>O and X ZnO (i.e., X = 0, 5, 10, 15, and 25 mol%). Several analytical methods for energy-dispersive X-ray (EDX) spectroscopy and Fourier transform infrared (FTIR) spectroscopy were used to characterise the prepared Zn5. The prepared ZnXs showed antibacterial effects against *Staphylococcus aureus*, *Bacillus cereus*, Methicillin-resistant *Staphylococcus aureus* (MRSA), and *Escherichia coli* strains. Also, the prepared Zn5 showed *in vitro* antibacterial activity in a wastewater sample from Mansoura wastewater treatment plant in Dakahlia, Egypt. Finally, the incorporation of Zinc (Zn5) enhanced the antibacterial effect of the prepared BBAGs sample on bacteria from a sewage wastewater sample. The research results discussed the possible environmental applies of Zn-doped borate bioactive glasses.

**keywords:** Wastewater, treatment, bacteria, borate-glass, zinc.

### 1.Introduction

Wastewater contains millions of different sorts of organisms, including the proteus group, anaerobic spore-forming bacilli, streptococci, staphylococci, and coliform, per milliliter. Wastewater is also a source of many pathogenic organisms that are harmful to people, including bacteria, viruses, and protozoa. Moreover, bacteriophages, a class of bacterial viruses, can be readily isolated from wastewater [1].

The community is at serious risk for illness due to the presence of microbial pathogens in contaminated, treated, and untreated waterways. Waterborne infections remain a major global health concern despite significant improvements in wastewater and water treatment. Over 250 million people are infected

with waterborne illnesses each year, and 10–20 million of them die as a result [2]. The high rate of infections in developing nations is largely due to factors such as less public health knowledge, socioeconomic status-related problems, and weaker hygienic standards than in more developed nations. The risk presented by many types of microbial pathogens in water necessitates the monitoring of sewage wastewater for these pathogens. To perform a suitable risk assessment, the kind and relative quantity of the microbial pathogens present must be determined. This is particularly important for treating and reusing wastewater [3].

Hench *et al.* (1971) first reported on bioactive modified soda lime silica glass, which is the oldest known bioactive material. Currently, it is a very well-characterized substance that has been applied to a number of biomedical fields [4].

By adding boron ions to the glass network in place of network silica ions, borate bioactive glasses (BBAGs) are created. The human body uses boron, an important trace element, for a number of purposes [5]. The body contains it as organoboron complexes, of which 96% are made up of boric acid and the remaining 4% are borate anion [6]. According to reports, a daily consumption of one mg of boron is ideal and necessary for the body to function normally. The body's largest concentration of boron is found in bone, nails, and hair [6].

Zinc (Zn) is a cofactor for several enzymes that facilitate the synthesis of proteins, which are required for DNA replication as well as the growth, differentiation, and multiplication of bone cells [7]. The biocompatibility and bioactivity of Zn-doped BBAGs have been studied [8,9]. Usually, ZnO acts as either a network modifier or an intermediate oxide based on the concentration at which it is included in a certain BBAG composition. The overall leaching behavior of the silicate matrix, which is controlled by the presence of ZnO in the glass structure, affects the reactivity of the glass surface when it comes into contact with physiological fluids.

The relative concentration of other oxides affects how Zn affects the characteristics of BBAGs in addition to Zn content [10]. Zn-doped BBAGs' antibacterial properties haven't been well studied. Certain mesoporous BBAGs, Other authors have discovered that Zn-doped BBAG and ZnO-based glass ceramics have antibacterial action against *S. aureus* [11], *S. epidermidis* and *Klebsiella pneumoniae* [12], *P. aeruginosa* and *Bacillus subtilis* [12,13], and *S. mutans* and *Actinomyces viscosus* [14].

## 2. Materials and methods

### 2.1. Preparation of ZnXs composite

The process of making BBAGs usually involves melting precursor oxide powders at temperatures higher than 1000 °C and rapidly cooling the resultant amorphous (non-

crystalline) glass in order to produce BBAGs as powders [15-17].

During the melt annealing process, silicates ( $\text{Si}_2\text{O}$ ) were totally substituted for borates ( $\text{B}_2\text{O}_3$ ) in equivalent amounts to create the BBAG composites [18].  $(75-X) \text{B}_2\text{O}_3$ ,  $10 \text{Na}_2\text{O}$ ,  $5 \text{P}_2\text{O}_5$ ,  $10 \text{Li}_2\text{O}$  and  $X \text{ZnO}$  (i.e.,  $X = 0, 5, 10, 15$ , and  $25 \text{ mol\%}$ ) was the composition that was employed. To create the glass ceramic, only chemically pure components were needed. The following substances were utilised to create  $\text{P}_2\text{O}_5$ ,  $\text{B}_2\text{O}_3$ ,  $\text{Na}_2\text{O}$ , and  $\text{ZnO}$ , respectively:  $\text{NH}_4\text{H}_2\text{PO}_4$ ,  $\text{H}_3\text{BO}_3$ ,  $\text{Na}_2\text{CO}_3$ , and  $\text{ZnO}$  [19,20].

To prepare the glass, a properly weighed batch is placed inside the platinum crucible and calcined for 30 minutes at 500°C. The main objective of the process is to remove water [19]. After that, it is melted in an electric oven at 1150 °C. Once the molten material has taken on the required shape, it will be cast into a stainless steel moulds. Lastly, the process will be carried out at 400 °C in the muffle furnace. After melt annealing the produced glass sample, The muffle was left to drop to room temperature at an average of 30 °C per hour [21,22].

### 2.2. Characterizations of Zn5 composite

#### 2.2.1. Fourier Transform Infrared (FTIR) spectroscopic analysis

FTIR transmittance was measured with Burker Vertex 80 (Germany) in the 400–4000  $\text{cm}^{-1}$  range. The materials were uniformly mixed with solid KBr for FTIR characterization, and then they were compressed for FTIR analysis, which was done in the instrument's chamber while it was being scanned [23].

#### 2.2.2. Energy-Dispersive X-ray (EDX) Spectroscopy

Energy Dispersive X-ray (EDX) was also measured using the Joel scanning electron microscope in order to determine the elemental composition of the synthesized borate glass composites (Zn5), where a beam of electrons collides (10–20 keV) on their surface. Following the electron beams collision, a picture was produced [24].

### 2.3. Antimicrobial activity assay

To find antimicrobial activity, the agar well diffusion technique was employed. 50  $\mu\text{L}$  of

sterile standard inoculum (*S. aureus* (ATCC6538), *B. cereus*, MRSA, and *E. coli* (ATC10536) was used to inoculate Luria-Bertani (LB) agar medium plates. Using a sterile corkborer, 6mm diameter wells were created in the LB agar medium, and 50 mg powder of ZnXs was added to each well. The inhibitory zone was evaluated after incubation for overnight at 37 °C [11]. Three duplicates of the tests were run, and the mean values were noted.

#### 2.4. Total count of bacteria in polluted sewage wastewater sample

Samples were gathered from Mansoura Wastewater Treatment Plant in Dakahlia Governorate. Zn5 impact on the overall count was examined and compared with samples of treated with 50 µg/mL of amoxicillin. In sterilized conical flasks, 0.1 g of Zn5 composite in 10 mL of sewage wastewater sample incubated at  $28 \pm 2^\circ\text{C}$ , 150 rpm for overnight.

100 µL suspension of wastewater samples, both before and after treatment, spread onto LB agar petri dishes in order to count the number of bacteria after incubation for overnight at 28 °C in 150 rpm shaking condition. Plates containing between 20 and 300 colonies are counted and documented as colony-forming units per milliliter, or CFU/mL [25].

### 3. Results and Discussion

#### 3.1. Characterizations of Zn5 Bioactive glass

##### 3.1.1. Fourier Transform Infrared (FTIR) spectroscopic analysis

A typical FTIR spectrum of the glass as-prepared, which contains 5 mol% zinc in borate bioglass, is depicted in **Fig. 1**. This spectrum shows broad absorption bands as a result of the general disorder in the network, which is primarily due to the wide distribution of structural units in this glass, as expected. The structure and dynamics of disorder materials have been extensively investigated using IR spectroscopy. A comprehension of the characteristics of vibration in a disordered system may be assisted through studying the infrared spectra of materials. The characterising peak at  $385\text{ cm}^{-1}$  and the identified band around  $410\text{ cm}^{-1}$  in the far infrared are indicative of the presence of ZnO and/or  $\text{Li}_2\text{O}$ . It is known that increasing network depolymerization is

accompanied by lower coordination numbers of the modifying cations, which may be attributed to the high field strength alkali and alkaline earth modifiers, as well as rare-earth sites in glasses [26-28]. Also, in high  $\text{Li}_2\text{O}$  content glasses with binary lithium borates, the 4-fold coordinated  $\text{Li}^+$  sites are prevalent [29]. Whereas, in binary Mg-borate glasses, it is predicted that  $\text{Mg}^{2+}$  oxygen tetrahedra will persist [30]. Next, an envelope that extends from approximately 600 to  $800\text{ cm}^{-1}$  is a characteristic of all spectacles. Given that the absorption band assigned at  $710\text{ cm}^{-1}$  may be associated with the bending of the B-O-B linkage [31]. Furthermore, network polyhedra exhibit stretching modes within the  $800\text{--}1650\text{ cm}^{-1}$  range. Typically, the region is divided into two regions. In the first region, tetrahedrally coordinated boron is responsible for the activity observed in the region between 800 and  $1100\text{--}1150\text{ cm}^{-1}$ . Thus, the borate matrix is responsible for the absorption bands at 858, 930, 1004, and  $1056\text{ cm}^{-1}$ , as reported by Pal, M., et al. (2011) [31]. Additionally, the band originates as a broad envelope with no discernible features; however, the spectrum with relatively high ZnO content is characterised by a distinct local maximum at  $1004\text{ cm}^{-1}$ . Contrary to the other region, which is located within the  $1100\text{--}1650\text{ cm}^{-1}$  range According to [32], the trigonal boron units that are active are responsible for the characteristic bands at 1208, 1356, and  $1587\text{ cm}^{-1}$  [33]. The FTIR spectrum investigations of the Zn system also indicate that the bands at 3789 and  $3718\text{ cm}^{-1}$  correspond to the stretching vibration modes of the hydroxyl group [33].

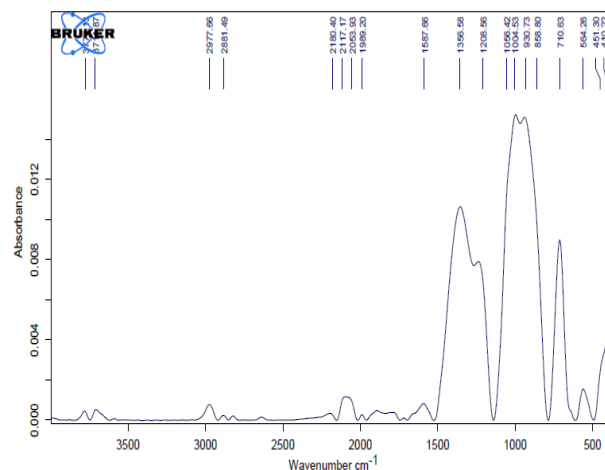


**Fig 1:** FTIR spectrum of the zinc borate (Zn5) sample.



### 3.1.2. Energy-Dispersive X-ray (EDX) Spectroscopy

It was employed to ascertain the elemental composition of zinc borates through energy dispersive spectroscopy (EDX). Zinc borate's EDX spectrum is illustrated in **Fig. 2**. The sample's elemental composition suggests the presence of oxygen, boron, sodium, phosphorus, and zinc. Possible explanations for the absence of the Li atom include the boron's overlap with its position. Previous studies reported that the sample's EDX spectrum is remarkably similar to other zinc borate structures [33,34]. The results acquired are consistent with the data obtained by the FTIR.

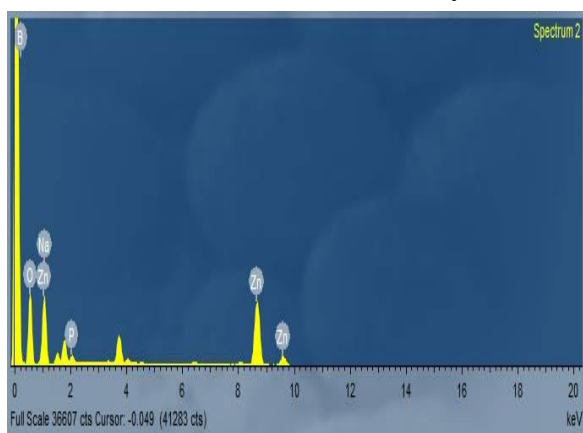


**Fig 2:** EDX spectrum of the zinc borate (Zn5) sample.

### 3.2. Biological evaluation of the prepared ZnXs composite

#### 3.2.1. Effect of the prepared ZnXs composite on the growth of pathogenic bacteria by well diffusion method

It has been highly suggested that bioactive glass be employed in place of the graft materials now in use [35].

It was discovered in this study that lowering the zinc oxide concentration in borate bioactive glass maximised the inhibitory impact of the produced ZnXs. In the case of *B. cereus*, as shown in **Fig. 3(a)** and **Table 1**, the borate particles in the free form from zinc oxide (Zn0) and the borate particles with the lowest concentration (5 mol%) of zinc oxide (Zn5) resulted in the development of the cells being inhibited, creating an inhibition zone of 16, 22 mm, respectively, whereas other ZnX composite (Zn10, Zn15, and Zn25) particles demonstrated no antibacterial action at the maximum amount of zinc oxide (10, 15, and 25

mol%). The prepared Zn0 demonstrated the highest activity with an inhibition zone of 10 mm in the case of *E. coli*, followed by Zn5 (8 mm), Zn10 (5 mm), Zn15, and Zn25 showed no antimicrobial activity at the highest concentration of zinc oxide (15 and 25 mol%, respectively), according to the results displayed in **Figs. 3 (b) and 4 (a) and Tables 1 and 2**. The findings displayed in **Fig. 3(c)** likewise demonstrated that, in the case of MRSA, only the produced Zn5 exhibited 11.5 mm inhibitory zones against bacterial growth. As seen in **Fig. 4(b) and Table 2**, the produced Zn10 and Zn15 demonstrated action against *S. aureus* with inhibition zones of 10 mm for both composites, but Zn25 showed no antimicrobial activity at the highest concentration of zinc oxide (25 mol%).

On the contrary, application of the produced ZnXs led to a rise in their antibacterial activity as the zinc oxide content dropped. Furthermore, the Zn0 and Zn5 composites with the lowest concentration of zinc oxide showed the highest antibacterial activity. The produced Zn-doped borate bioactive glass composites exhibited significant inhibition of the bacterial strains tested. The effect that the presence of zinc and boron ions produces can be used to explain this.

**Table 1:** Inhibition zone (mm) of pathogenic bacterial growth after treatment with Zn0 and Zn5 samples.

Pathogens	Inhibition Zone (mm*)	
	Zn0	Zn5
<i>B. Cereus</i>	16 ± 0.83	22 ± 0.66
<i>E. coli</i>	10 ± 0.77	8 ± 0.33
<i>MRSA</i>	N. A	11.5

\* Values are average (n=3), NA: Not active.

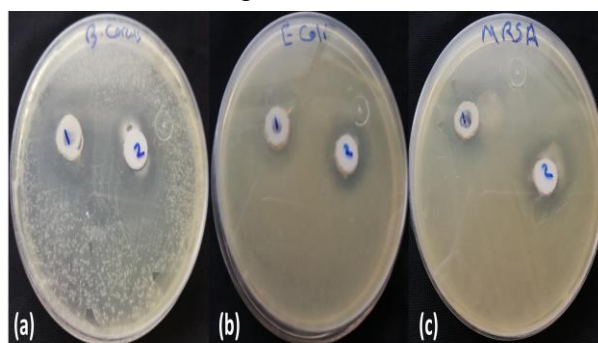


**Fig 3:** Antibacterial activity of Zn0 (1) and Zn5 (2) against *B. Cereus* (a), *E. coli* (b), and MRSA (c) by the agar well-diffusion method on LB agar media.

**Table 2:** Antimicrobial activity of the prepared Zn10, Zn15 and Zn5 by agar well diffusion method against some pathogenic bacteria.

Pathogen	Inhibition Zone (mm*)		
	Zn10	Zn15	Zn25
<i>E. coli</i>	5 ± 0.88	N. A	N. A
<i>S. aureus</i>	10 ± 0.63	10 ± 0.82	N. A

\* Values are average (n=3), NA: Not active.

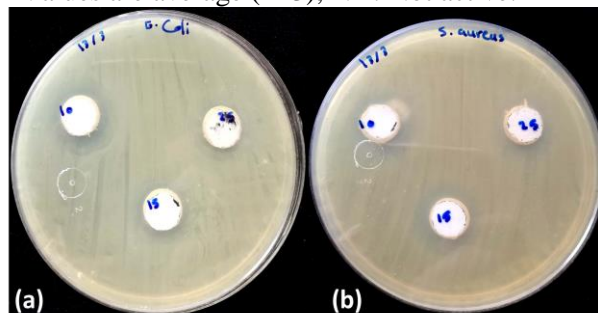


**Fig 4:** Antibacterial activity of the prepared Zn10 (10), Zn15 (15), and Zn25 (25) against *E. coli* (a), and *S. aureus* (b) by the agar well-diffusion method on LB agar media.

### 3.2.2. Effect of Zn5 composite on sewage wastewater

Zn5 composite, with the lowest concentration of zinc oxide, showed the highest antibacterial activity, so it is used in the treatment of wastewater. As demonstrated in **Fig. 5**, the prepared Zn5's good attitude as an antibacterial agent was reflected in the decrease in the number of bacterial colonies. Moreover, the colony count of cultures produced with or without the generated Zn5 composite was used to examine the cell viability of the harmful bacteria in wastewater. The findings displayed in **Fig. 5** unequivocally showed that the sample treated with amoxicillin, a broad-spectrum antibiotic, had a significantly lower number of viable bacterial cells following incubation with the produced Zn5 composite (positive control). Furthermore, the medium's pH was adjusted from 8.0 to 9.3.

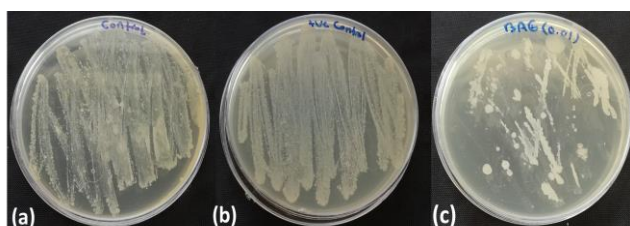


**Fig 5:** Effect of the prepared Zn5 on the bacteria from wastewater sample; before the treatment (a) and after the treatment by Amoxicillin (b) and Zn5 (c).

In general, the outcomes showed that the bioactive glass composite that worked the best was the prepared Zn-doped borate bioactive glass containing 5 mol% of ZnO (Zn5), followed by Zn0, Zn10, Zn15, and Zn25. Conversely, lowering the zinc oxide concentration increased the inhibitory effect of all composite types tested, resulting in a strong antibacterial effect with boron. The medium's pH, which modifies the surrounding media's pH, was one of the suggested causes of this antibacterial effect [18]. In a related study, the growth of *E. coli*, *Shigella sonnei*, *Vibrio natriegens*, *Staphylococcus epidermidis*, *Serratia marcescens*, and methicillin-resistant *S. aureus* was inhibited by borate ( $B_2O_3$ ) alone [36].

### 4. References

1. Wu, B., R. Wang, and A.G. Fane, (2017) The roles of bacteriophages in membrane-based water and wastewater treatment processes: A review. *Water research*,. **110**: p. 120-132.
2. Kristanti, R.A., et al., (2022) Microbiological contaminants in drinking water: Current status and challenges. *Water, Air, & Soil Pollution*,. **233**(8): p. 299.
3. Nguyen, A.Q., et al., (2021) Monitoring antibiotic resistance genes in wastewater treatment: Current strategies and future challenges. *Science of the Total Environment*,. **783**: p. 146-964.
4. Karasu, B., et al., (2017) Bioactive glasses. *El-Cezerî Journal of Science and Engineering*,. **4**(3): p. 436-471.
5. Swager, T.M. and S.P. Luppino, (2015) Nothing boring about this borylation. *Synfacts*,. **11**(03): p. 0266-0266.
6. Uluisik, I., H.C. Karakaya, and A. Koc, (2018) The importance of boron in biological systems. *Journal of Trace Elements in Medicine and Biology*,. **45**: p. 156-162.
7. Chasapis, C.T., et al., (2020) Recent aspects of the effects of zinc on human health. *Archives of toxicology*,. **94**: p. 1443-1460.
8. Neščáková, Z., et al., (2021) Polymer (PCL) fibers with Zn-doped mesoporous bioactive glass nanoparticles for tissue regeneration. *International Journal of*

9. Neščáková, Z., et al., (2019) Multifunctional zinc ion doped sol-gel derived mesoporous bioactive glass nanoparticles for biomedical applications. *Bioactive materials*,. **4**: p. 312-321.
10. Balasubramanian, P., et al., (2015) Zinc-containing bioactive glasses for bone regeneration, dental and orthopedic applications. *Biomedical glasses*,. **1**(1).
11. El-Baz, F.K., et al., (2015) Antiviral-antimicrobial and schistosomicidal activities of Eucalyptus camaldulensis essential oils. *Int J Pharm Sci Rev Res*,. **31**(1): p. 262-8.
12. Riaz, M., et al., (2015) In vitro antimicrobial activity of ZnO based glass-ceramics against pathogenic bacteria. *Journal of Materials Science: Materials in Medicine*,. **26**: p. 1-12.
13. Atkinson, I., et al., (2016) Influence of ZnO addition on the structural, in vitro behavior and antimicrobial activity of sol-gel derived CaO-P<sub>2</sub>O<sub>5</sub>-SiO<sub>2</sub> bioactive glasses. *Ceramics International*,. **42**(2): p. 3033-3045.
14. Boyd, D., et al., (2006) The antibacterial effects of zinc ion migration from zinc-based glass polyalkenoate cements. *Journal of Materials Science: Materials in Medicine*,. **17**: p. 489-494.
15. da Silva, L.C.A., et al., (2021) The role of Ag<sub>2</sub>O on antibacterial and bioactive properties of borate glasses. *Journal of Non-Crystalline Solids*,. **554**: p. 120-611.
16. Naseri, S., et al., (2022) Silver-doped sol-gel borate glasses: Dose-dependent effect on Pseudomonas aeruginosa biofilms and keratinocyte function. *Journal of the American Ceramic Society*,. **105**(3): p. 1711-1722.
17. Rahimnejad Yazdi, A., et al., (2018) The impact of gallium content on degradation, bioactivity, and antibacterial potency of zinc borate bioactive glass. *Journal of Biomedical Materials Research Part B: Applied Biomaterials*,. **106**(1): p. 367-376.
18. Al-Rashidy, Z., et al., (2017) Aqueous electrophoretic deposition and corrosion protection of borate glass coatings on 316 L stainless steel for hard tissue fixation. *Surfaces and Interfaces*,. **7**: p. 125-133.
19. Brauer, D.S., (2015) Bioactive glasses-structure and properties. *Angewandte Chemie International Edition*,. **54**(14): p. 4160-4181.
20. Yao, A., et al., (2007) In vitro bioactive characteristics of borate-based glasses with controllable degradation behavior. *Journal of the American Ceramic Society*,. **90**(1): p. 303-306.
21. Kamal, H. and A. Hezma, (2018) Structure and physical properties of borosilicate as potential bioactive glasses. *Silicon*,. **10**(3): p. 851-858.
22. Kamal, H., (2014) Structure and physical properties of silver borate bioactive glasses. *Res. J. Pharm. Biol. Chem. Sci*,. **5**.
23. Kamal, H. and A. Abdelghany, (2015) Effect of transition metal addition in the bioactivity of borate bioglass dental materials. *The Journal of Dentist*,. **3**: p. 11-21.
24. Aguilar-Perez, F.J., et al., (2016) Preparation and bioactive properties of nano bioactive glass and segmented polyurethane composites. *Journal of biomaterials applications*,. **30**(9): p. 1362-1372.
25. March, S.B. and S. Ratnam, (1986) Sorbitol-MacConkey medium for detection of Escherichia coli O157: H7 associated with hemorrhagic colitis. *Journal of clinical microbiology*,. **23**(5): p. 869-872.
26. Hoppe, U., et al., (2005) Structure of rare-earth phosphate glasses by X-ray and neutron diffraction. *Journal of non-crystalline solids*,. **351**(40-42): p. 3179-3190.
27. Abdelghany, A.M., F.H. ElBatal, and H.A. ElBatal, (2014) Zinc containing borate glasses and glass-ceramics: search for biomedical applications. *Processing and application of ceramics*,. **8**(4): p. 185-193.
28. Topper, B. and D. Möncke, (2022) Structure and Properties of Borate Glasses..
29. Kamitsos, E.I., et al., (1990) Infrared reflectance spectra of lithium borate glasses. *Journal of Non-Crystalline Solids*,. **126**(1-2): p. 52-67.

30. Kamitsos, E., M. Karakassides, and G.D. Chryssikos, (1987) Vibrational spectra of magnesium-sodium-borate glasses. 2. Raman and mid-infrared investigation of the network structure. *Journal of Physical Chemistry*,. **91**(5): p. 1073-1079.
31. Pal, M., B. Roy, and M. Pal, (2011) Structural characterization of borate glasses containing zinc and manganese oxides. *Journal of Modern Physics*,. **2011**.
32. Topper, B., et al., (2023) Zinc borate glasses: properties, structure and modelling of the composition-dependence of borate speciation. *Physical Chemistry Chemical Physics*,. **25**(8): p. 5967-5988.
33. Savrik, S.A., et al., (2018) Nano zinc borate as a lubricant additive, in *Applied Physical Chemistry with Multidisciplinary Approaches*, Apple Academic Press. p. 303-323.
34. Salatein, N.M., et al., (2024) Improving the physical and optical characteristics of Zinc doped borate glass for bone replacement. *Optical and Quantum Electronics*,. **56**(1): p. 3-10.
35. Ottomeyer, M., et al., (2016) Broad-spectrum antibacterial characteristics of four novel borate-based bioactive glasses..
36. Liu, X., et al., (2010) Bioactive borate glass scaffolds: in vitro and in vivo evaluation for use as a drug delivery system in the treatment of bone infection. *Journal of Materials Science: Materials in Medicine*,. **21**: p. 575-582.